Laminar and turbulent forced convection in accelerating and decelerating curved flows

H. Umur* and A. A. Ozalp

Department of Mechanical Engineering, Uludag University, 16059, Gorukle, Bursa, Turkey

This article is concerned with accelerating and decelerating flows over straight, concave and convex surfaces encompassing laminar and turbulent boundary layers. Flow and heat transfer experiments were carried in a blowing-type, low-speed wind tunnel and measurements indicated that the concave curvature and acceleration caused thinner boundary layers and augmented heat transfer rates, whereas the convex wall and deceleration resulted in the contrary. A new empirical equation is derived to model the combined effects of boundary layer development, surface curvature and pressure gradient on surface heat transfer values, which coincides with the experimental data within a deviation range of ± 3%.

THE continuing interest in flows and heat transfer over flat plate, concave and convex surfaces stems from their possible effects in turbine blades of jet engines, vehicle aerodynamics, aircraft wings, submarines, spaceships, cooling lines of power plants, etc. Flow phenomena in all cases are mainly subjected to pressure gradients (favourable or adverse), surface curvature and a wide range of Reynolds numbers.

There have been many previous investigations of flow and heat transfer in flat plate boundary layers with pressure gradients. For instance, investigations of Abu Ghannam and Shaw[1], Zhou and Wang[2], and Fukagata *et al.*[3] were concerned with transition to turbulent flow and Reynolds stress distribution, while those of Taylor *et al.*[4], Rivir *et al.*[5], Kasagi[6], and Umur and Karagoz[7] dealt with the augmentation of heat transfer with/without streamwise pressure gradients.

Investigations with concave curvature have focused mainly on the effects of the Görtler instability, curvature and pressure gradients on transition and heat transfer. Crane and Sabzvari[8], Barlow and Johnston[9], Inagaki and Aihara[10], Volino and Simon[11], and Flack and Johnston[12] dealt with the Görtler instability and transition. On the other hand, Ligrani *et al.*[13], Umur[14], Wright and Schobeiri[15], and Umur[16] have concentrated on heat transfer augmentation with curvature and pressure gradients.

The investigations of Muck *et al.*[17], Wang and Simon[18], Plesniak *et al.*[19] and Webster *et al.*[20] were concerned with the stabilizing effect of convex curvature and flow transition, while that of Ligrani and Hedlund[21] presented pressure gradient and curvature effects on heat transfer.

The measurements reported here were obtained on three different (straight, concave and convex) surfaces for initial free stream momentum thickness Reynolds numbers from 200 to 2000, with longitudinal pressure gradients of k_x values from –0.47 to +0.47, encompassing laminar and turbulent flows. They include local values of velocity, surface temperature and wall heat transfer coefficient in terms of Stanton numbers. They show the combined effects of pressure gradient and surface curvature on heat transfer augmentation. The stabilizing effects of favourable pressure gradients and convex curvature and the destabilizing effects of adverse pressure gradients and concave curvature on flows and heat transfer are also extensively examined here. Flow conditions and instrumentation are described in the following section and the results are presented and discussed in the third section. The article ends with a summary of the more important findings.

Flow conditions and instrumentation

Flow and heat transfer measurements were carried out in test sections of straight, concave and convex curvatures mounted on a blowing-type, low-speed wind tunnel (Figure 1). An area contraction of 3 provided an air velocity of 30 m/s to a rectangular test section of 750 mm in length for flat and 1000 mm in length for concave and convex walls with a radius of 1500 mm. Honeycomb and screen packs in the upstream of the contraction ensured absence of swirl. A straight plate of 400 mm in length was also installed in the upstream of the test section to allow the boundary layer growth prior to the test section. An adjustable upper wall ensured the desired streamwise distance favourable or adverse pressure gradients, in terms of the velocity gradient parameter $k = (\nu/U^2)(dU/dx)$ where ν is the kinematic viscosity in m^2/s; U is the mean free stream velocity in m/s and x is the streamwise direction, from -3.6×10^{-6} to $+3.6 \times 10^{-6}$ in laminar and from -0.6×10^{-6} to $+0.6 \times 10^{-6}$ in turbulent flows, corresponding to streamwise pressure gradient $k_x = (x/U)(dU/dx)$ from –0.47 to +0.47 in either flow. The k values were tried to be kept constant along the downstream and hence the k_x values were recalculated for each streamwise location within ± 5%. The sign of pressure gradient parameter was taken (+)

*For correspondence. (e-mail: umur@uludag.edu.tr)

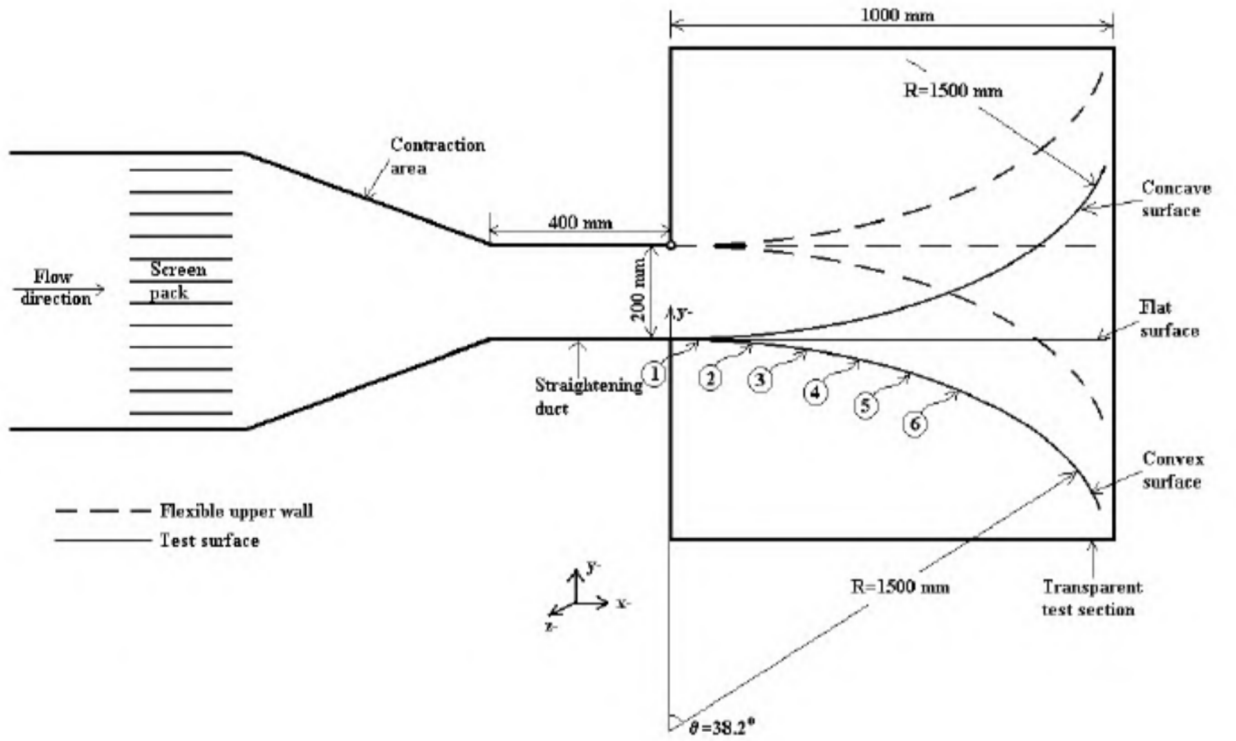

Figure 1. Test section.

for accelerating and (–) for decelerating flows. Mean velocity profiles in the pitchwise direction for all locations were measured by a semi-rectangular pitot tube connected to the static pressure tappings and a micromanometer, which resulted in a total measurement error of less than ± 4%. Wall temperatures were recorded by copper-constantan thermocouples on straight, concave and convex walls. The copper plate test wall was heated by an electrical resistance (a high-current, low-voltage transformer) to provide a near-constant heat flux condition, which provided uniform wall temperature distribution in streamwise direction within ± 0.5°C throughout the measurements. The heat loss through the backside of the walls was minimized by fibreglass insulation and convection heat loss was estimated from the difference between the powers required to maintain locally constant wall temperature with and without flow.

Results and discussion

This section presents velocity profiles and heat transfer characteristics over flat plate, concave and convex walls with longitudinal pressure gradients in laminar and turbulent flows. The preliminary measurements showed laminar boundary layer characteristics at 3 m/s and turbulent at 15 m/s on the basis of a variety of evidence, i.e. velocity profile, shape factor H, streamwise distance Reynolds number Re_x, momentum thickness Reynolds number Re_θ (where θ is the momentum thickness in m) and Stanton number St. Experiments on three test sections have been carried out with zero pressure gradient ($k = k_x = 0$) and non-zero pressure gradients, i.e. $k = \pm 2.0 \times 10^{-6}$ and $\pm 3.6 \times 10^{-6}$ in laminar and $k = \pm 0.4 \times 10^{-6}$ and $\pm 0.6 \times 10^{-6}$ in turbulent flows, corresponding to the same k_x values of ± 0.26 and ± 0.47 in both cases respectively. Measurements of velocities and wall temperatures in cross-stream variation showed no significant change, so that all results were presented in the pitchwise and streamwise directions.

Flat plate measurements

All velocity measurements were presented in non-dimensional form, u/U where u is the streamwise velocity in m/s, at downstream stations of 60, 180, 420 and 660 mm. Laminar velocity profiles at 3 m/s (Figure 2 *a*), show that the large differences in profile shape between the strongest favourable pressure gradient of 3.6×10^{-6} and the lowest adverse pressure gradient of -3.6×10^{-6} occurred, particularly at the last station of 660 mm, where the accelerating mean velocity was almost threefold of the decelerating one. The initial boundary layer thickness of around 13 mm for all pressure gradients corresponded to a streamwise distance Reynolds number ($Re_x = Ux/\nu$) of 245,000 based on the Blasius solution of $\delta/x = 5/Re_x^{0.5}$ (where δ is

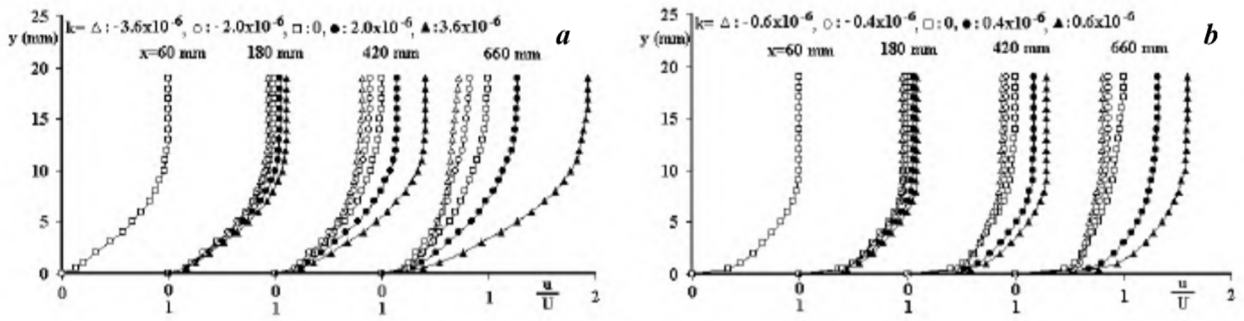

Figure 2. Flat surface velocity profiles in (*a*) laminar and (*b*) turbulent flows.

the boundary layer thickness in m) and a momentum thickness Reynolds number ($Re_\theta = U\theta/\nu$) of 280 and a shape factor (H) of 2.75. The same initial values of δ, Re_x, Re_θ and H at x of 60 mm, for each case, showed that boundary layer development had not been yet influenced by pressure gradients (favourable or adverse). The thicker δ due to decelerating flows, particularly at last stations, caused higher corresponding boundary layer parameters that can be attributed partly to the destabilizing effect of adverse gradients. The turbulent velocity measurements at 15 m/s (Figure 2 *b*), have been obtained with k values of 0, $\pm 0.4 \times 10^{-6}$ ($k_x = \pm 0.26$) and $\pm 0.6 \times 10^{-6}$ ($k_x = \pm 0.47$), which are far from the relaminarization parameter of 3.2×10^{-6}. The more resistant turbulent boundary layers to adverse gradients resulted in smaller δ than those of laminar flow. The same boundary layer parameters of δ, Re_x, Re_θ and H for all pressure gradients indicated that there was no influence of pressure gradients initially, like in the previous case. The turbulent flow characteristics of 15 m/s all over the surface is in accord with Rivir *et al.*[5] and Cheng *et al.*[22], who confirmed turbulent flows for the entire measurement region.

All experimental Stanton numbers, defined by $St = h/(\rho U C_p)$, where h is the convective heat transfer coefficient in W/m^2K, were compared with each other and with the analytical flat plate solution for constant heat flux, $St = 0.453 Re_x^{-0.5} Pr^{-2/3}(1-(x_1/x)^{0.75})^{-1/3}$, where x is the virtual streamwise distance, Pr is the Prandtl number, x_1 is the unheated starting length, $h = q/(T_w - T_o)$; where q is the heat flux in W/m^2, T_w is the wall temperature in °C and T_o is the free stream temperature in °C. $q = q_F - q_o$, q_F and q_o refer to flow-on and off powers, ρ and C_p are the density and specific heat of fluid. In this particular case, the cumulative uncertainty of the experimental Stanton number is directly estimated by the equation

$$\frac{\partial St}{St} = \left[\left(\frac{\partial U}{U}\right)^2 + \left(\frac{\partial q}{q}\right)^2 + \left(\frac{\partial T}{T}\right)^2 + \left(\frac{\partial \rho}{\rho}\right)^2 + \left(\frac{\partial C_p}{C_p}\right)^2 \right]^{1/2}$$

and hence the maximum uncertainty in heat transfer measurements is found to be ± 5%.

The measured Stanton numbers (Figure 3 *a*), in near-zero pressure gradient were in accord with laminar solution, and increased by an amount of 27% with the strongest pressure gradient and decreased by 31% with the lowest pressure gradient, as seen extensively in Table 1, which is inconsistent with the experimental results of Zhou and Wang[2], who reported augmented St by 8%, only at a significant location, for $k = 4.1 \times 10^{-6}$, which is much stronger than the present extreme pressure gradient. The higher and lower heat transfer coefficients in laminar region and corresponding Stanton numbers resulted mainly from the reduced boundary layer thickness with fuller velocity profiles due to acceleration and thicker boundary layer owing to deceleration than that of zero gradient respectively.

The measured turbulent Stanton numbers for $k_x = 0$ are around the turbulent flat plate correlation formula of $St = 0.03 Re_x^{-0.2} Pr^{-0.4}(1-(x_1/x)^{0.9})^{-1/9}$ all over the surface, and Stanton numbers rose by 14% for $k_x = 0.26$ ($k = 0.4 \times 10^{-6}$) and fell by 15% for $k_x = -0.26$ ($k = -0.6 \times 10^{-6}$). The stabilizing influence of the strongest pressure gradients of $k_x = 0.47$ and the destabilizing effect of the lowest gradients of $k_x = -0.47$ on Stanton number variations became more pronounced, particularly towards the downstream regions where St rose by 29% and fell by 27% with respect to zero pressure gradient values respectively, as seen comprehensively in Table 1. These experimental results are contrary to the numerical findings of Umur and Karagoz[7], who showed turbulent St to decrease with acceleration, unlike laminar flows. However, in the numerical procedure of Umur and Karagoz[7], the turbulent flow was considered as fully developed and the influence of acceleration on boundary layer development was not taken into account, where the combined effects of these approaches can produce significant variations in heat transfer rates. All experimental Stanton numbers have also been plotted in Figure 3 *b* as a function of k_x based on constant Re_x curves, so as to explain much more explicitly St increase with favourable pressure gradient and St decrease with adverse pressure gradient, both in laminar and turbulent flows. All measured values were also compared with the new empirical equation, which is valid

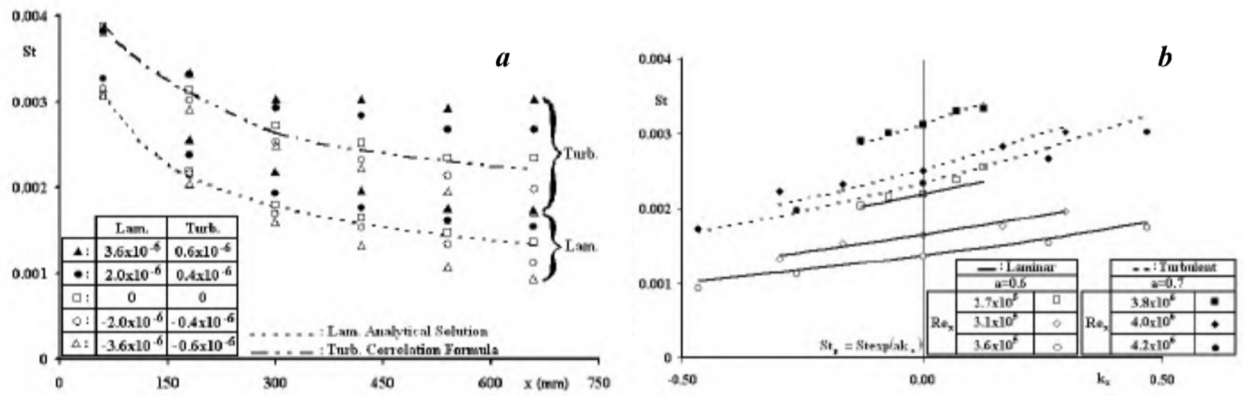

Figure 3. Variation of flat surface Stanton numbers (***a***) in streamwise direction and (***b***) with pressure gradients.

Table 1. Flat surface St rates with respect to those of flat plate $k_x = 0$

k_x	–0.47	–0.26	0	0.26	0.47
Laminar (%)	–31	–18	0	13	27
Turbulent (%)	–27	–15	0	14	29

from $k_x = -1.0$ to 1.0, for the estimation of both laminar and turbulent Stanton numbers. The estimation of Stanton number under the influence of pressure gradients (St_p) is defined here as

$$St_p = St\exp(ak_x), \quad (1)$$

where the equation parameter a becomes 0.6 for laminar and 0.7 for turbulent flows. The exponential term of eq. (1) defines the dependence of heat transfer rates on streamwise pressure gradients and the empirical values (Figure 3 *b*) show parallelism with the experimental data with a maximum error of ± 3%.

Concave surface measurements

The velocity profiles of Figure 4 *a* at 3 m/s show laminar initial boundary layer parameters of $\delta = 11$ mm and corresponding values of $Re_x = 175{,}000$, $Re_\theta = 230$, $G_\theta = 6.5$, where G_θ is the Görtler number ($G_\theta = Re_\theta(\theta/R)^{0.5}$) and R is the surface curvature in m, and $H = 2.55$ for all gradients. The concave wall parameters became smaller with acceleration and greater with deceleration than those of the flat plate. Görtler number has also been taken into account to describe the boundary layer of concave surfaces as a primary factor. The laminar boundary layer development along the curvature seemed to be more vulnerable to adverse pressure gradient than flat plate flow. The combined destabilizing effects of concave curvature and adverse gradient became much more remarkable, particularly towards the end of the curvature where the free stream velocity difference between the strongest favourable and the lowest adverse gradients is larger than that for the flat surface, similar to those of Volino and Simon[11]. The turbulent velocity measurements at 15 m/s (Figure 4 *b*) were found to be more resistant to adverse gradients than laminar flows. The initial turbulent boundary layer parameters of δ, Re_θ, G_θ and H were 8 mm, 1100, 30 and 1.5 at all pressure gradients respectively, which show turbulent flow characteristics and are similar to those of So and Mellor[23], and Kestoras and Simon[24].

Experimental Stanton numbers (Figure 5 *a*) were compared with each other and the new empirical equation was obtained as follows:

$$St_c = St\left[1 \pm \left(\frac{\theta_{loc}}{\theta_{in}}\right)^b \left(\frac{\theta_{in}}{R}\right)^c\right], \quad (2)$$

where St_c is the concave or convex wall St with no pressure gradient, θ_{in} is the initial momentum thickness in mm and θ_{loc} is the local momentum thickness in mm. Equation (2) is applicable to both concave and convex surfaces. In eq. (2) $R \to \infty$ for flat wall, (+) refers to concave surface and (–) to convex surface. For concave surface, b is 1.75 and 3.5, and c is 0.2 and 0.33 in laminar and turbulent flows respectively. The experimental Stanton numbers for zero pressure gradient are in good agreement with eq. (2), with an uncertainty of less than ± 2%. The thinner δ in favourable gradients and thicker δ in adverse gradients resulted in higher and lower Stanton numbers respectively. St increased with favourable gradients in the downstream and reached a peak value at the last station, where St rose by 16% and 36% at $k = 2.0 \times 10^{-6}$ and 3.6×10^{-6} ($k_x = 0.26$ and 0.47) and St fell by 11% and 26% at $k_x = -0.26$ and –0.47 with respect to zero pressure gradient, as seen in Table 2 respectively. The concave wall heat transfer enhancement with the highest acceleration exceeded that of flat plate zero pressure gradient values by a factor of more than 2.3, which is in good agreement

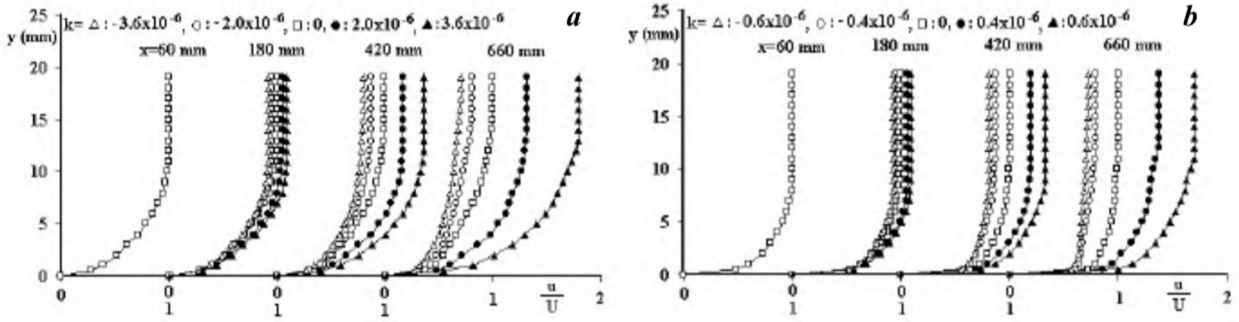

Figure 4. Concave surface velocity profiles in (*a*) laminar and (*b*) turbulent flows.

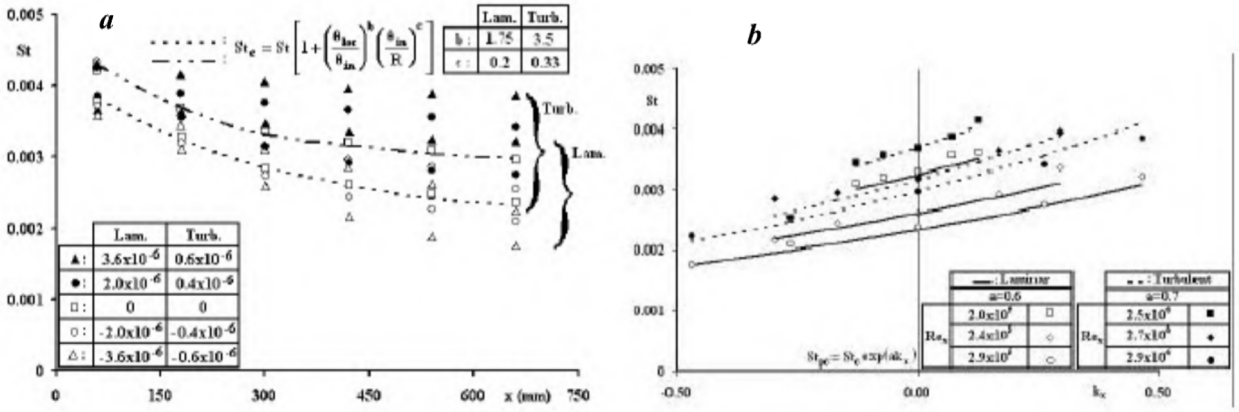

Figure 5. Variation of concave surface Stanton numbers (*a*) in streamwise direction and (*b*) with pressure gradients.

Table 2. Concave surface St rates

	With respect to those of concave wall $k_x = 0$		With respect to those of flat plate $k_x = 0$	
k_x	Laminar (%)	Turbulent (%)	Laminar (%)	Turbulent (%)
–0.47	–26	–25	29	–4
–0.26	–11	–14	54	9
0	0	0	74	27
0.26	16	15	102	46
0.47	36	30	136	65

with Umur[14], who recorded more than 200% augmentation in St on stronger concave curvature due to Görtler vortices, and larger than those of Wright and Schobeiri[15], who showed about 30% increase due to curvature. Turbulent Stanton numbers, compared with concave wall values of $k_x = 0$, rose by 15% and 30% for $k = 0.4 \times 10^{-6}$ and 0.6×10^{-6} ($k_x = 0.26$ and 0.47) and fell by 14% and 25% for $k_x = -0.26$ and –0.47, particularly towards the end of curvature (Table 2), respectively.

The turbulent St with favourable pressure gradient (Table 2), increased by 65% above the flat plate values of $k_x = 0$, which is slightly higher than those of Umur[14], and Ligrani and Hedlund[21], and less than that of Kottke[25], who reported 80% heat transfer enhancement in the upstream flow. The higher concave wall St rates over flat plate values resulted mainly from the concave curvature and partly from favourable gradients. The experimental Stanton numbers were also presented as a function of k_x (Figure 5 *b*), so as to explain more noticeably $\mathrm{St} = f(k_x)$, both in favourable and adverse pressure gradients such that eq. (2) is modified accordingly:

$$\mathrm{St}_{pc} = \mathrm{St}_c \exp(ak_x), \tag{3}$$

where St_{pc} is the concave or convex wall St with pressure gradient.

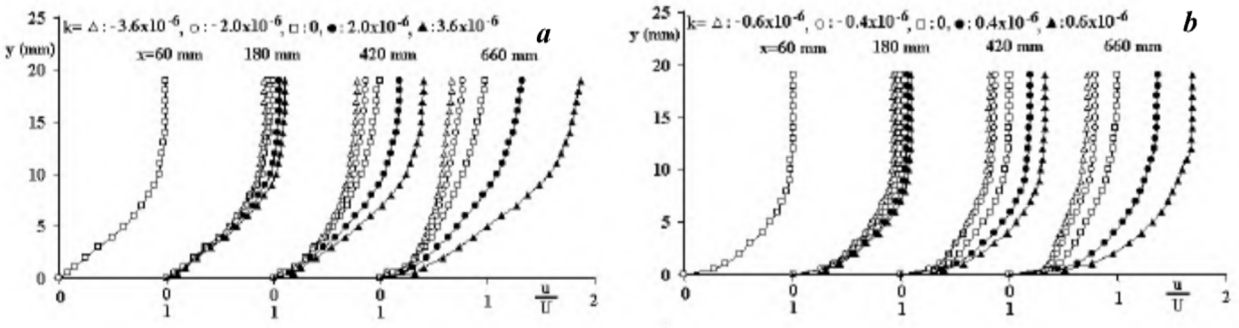

Figure 6. Convex surface velocity profiles in (*a*) laminar and (*b*) turbulent flows.

Table 3. Convex surface St rates

	With respect to those of convex wall $k_x = 0$		With respect to those of flat plate $k_x = 0$	
k_x	Laminar (%)	Turbulent (%)	Laminar (%)	Turbulent (%)
–0.47	–19	–28	–45	–43
–0.26	–13	–13	–41	–31
0	0	0	–32	–21
0.26	10	12	–25	–12
0.47	22	24	–17	–2

The close relationship between the measured values and the empirical equation curves of Figure 5 *b* shows that the proposed eq. (3) together with eq. (2) can successfully be used for the estimation of concave wall St with pressure gradients within a deviation of less than ± 3%.

Convex surface measurements

Convex wall velocity profiles at 3 m/s are illustrated in Figure 6 *a* with an initial boundary layer thickness of 14 mm and corresponding higher values of $Re_x = 285{,}000$, $Re_\theta = 360$ and $H = 2.95$ than those of the previous cases. The lowest gradient of -3.6×10^{-6}, together with the convex wall made the flow more vulnerable than those of the flat plate and concave surface and caused a slight sign of inflection, especially towards the end of curvature. The thicker boundary layer than that of the flat plate at 3 m/s simply exhibits the stabilizing effect of convex curvature that delays the destabilizing effect of adverse gradients. The turbulent velocity profiles at 15 m/s are plotted in Figure 6 *b*, which show the maximum deviation between the exit free stream velocities of the strongest and the lowest gradients, towards the end of curvature. The more resistant velocity profiles to the adverse gradients showed no trends of distortion in profiles, as if everything was buried in the viscous sublayer. The initial turbulent boundary layer parameters of $\delta = 12$ mm, $Re_\theta = 1600$ and $H = 1.6$ and those of downstream values are larger than the turbulent values of straight and concave walls, as expected, because of the stabilizing effect of convex curvature, similar to those of Muck *et al.*[17] and Webster *et al.*[20], who reported turbulent flows at 15 m/s on the entire convex surface.

Convex wall measured Stanton numbers in zero pressure gradient remained around eq. (2) (Figure 7 *a*), in laminar and turbulent flows respectively. Here *b* and *c* in eq. (2) get the values of 3 and 0.4 in laminar and of 6 and 0.5 in turbulent flows. Stanton numbers increased with favourable pressure gradients by 10% and 22% at $k = 2.0 \times 10^{-6}$ and 3.6×10^{-6} ($k_x = 0.26$ and 0.47) (Table 3), with respect to zero gradient values which are in accord with Wang and Simon[18] and Turner *et al.*[26], who reported an increase on convex wall due to favourable gradients. For adverse pressure gradient, St decreased by 13% and 19% at $k_x = -0.26$ and –0.47 respectively, below that of zero pressure gradient, as in the previous straight and concave wall measurements. The lowest pressure gradient with convex curvature corresponds to 45% smaller St values than those of flat plate zero pressure gradient (Table 3).

Turbulent Stanton number enhancement due to acceleration was 12% and 24% for $k = 0.4 \times 10^{-6}$ and 0.6×10^{-6} ($k_x = 0.26$ and 0.47) above that of zero gradient, similar to the results of Ligrani and Hedlund[21], and Turner *et al.*[26]. Convex wall Stanton number in decelerating case fell by 13% and 28% for $k_x = -0.26$ and –0.47 below that of zero gradient. The total Stanton number reduction due to convex curvature and to the lowest adverse pressure gradient is 43% below the flat plate values of zero pressure gradient (Table 3). The decrease in Stanton number due to convex curvature was also reported by Wang and Simon[18], who

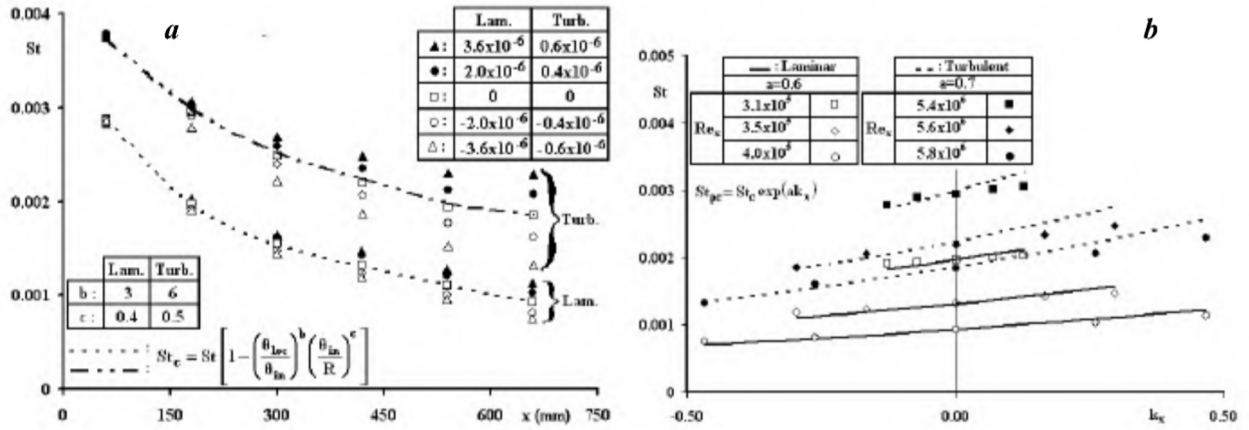

Figure 7. Variation of convex surface Stanton numbers (*a*) in streamwise direction and (*b*) with pressure gradients.

concluded that stronger convex curvature decreased heat transfer values in laminar, transition and turbulent regions. The augmentation of measured Stanton numbers from adverse to favourable can also easily be seen in Figure 7 *b* as a function of $\exp(ak_x)$, and all experimental values are in good agreement with eq. (3) in either pressure gradients. These experimental results show that eq. (3) together with eq. (2) can successfully be applied to all types of external flows in order to estimate the Stanton numbers with an ambiguity of less than ± 3%.

Conclusion

The thinner boundary layers due to concave curvature and acceleration give rise to higher heat transfer augmentation and thicker boundary layers owing to convex curvature and deceleration to smaller heat transfer rates both in laminar and turbulent flows. For the flat surface, the strongest acceleration caused Stanton number to increase by up to 29% in both flow conditions and the lowest deceleration to decrease by 31% in laminar and by 27% in turbulent flows. For the concave surface, the augmentation of Stanton number was 36% and 30% in laminar and turbulent accelerating flows and fell around 25% in both flows compared to that of zero pressure gradient. For the convex surface, Stanton numbers increased up to 22% and 24% in the strongest and decreased down to 19% and 28% in the lowest pressure gradients with respect to zero pressure gradient in laminar and turbulent flows respectively. On the other hand, Stanton number with respect to the flat plate values increased up to 74% and 27% due to concave curvature itself and decreased down to 32% and 21% owing to convex curvature in laminar and turbulent flows respectively. The Stanton number, due to both concave curvature and strongest acceleration, exceeded that of the zero pressure gradient flat plate values by a factor of 2.4 and 1.65 in laminar and turbulent flows respectively. Furthermore, the lowest St in the convex wall decelerating flows remained around 45% below that of the flat plate zero pressure gradient in both flows. The new proposed equations can successfully be applied to all surface types for the estimation of accelerating and decelerating flow Stanton numbers, with a maximum deviation of ± 3% from the experimental data, provided that the parameters of θ, R and k_x are defined properly.

1. Abu Ghannam, B. J. and Shaw, H., Natural transition of boundary layers – The effects of turbulence, pressure gradient and flow history. *J. Mech. Eng. Sci.*, 1980, **22**, 213–228.
2. Zhou, D. and Wang, T., Combined effects of elevated free-stream turbulence and streamwise acceleration on flow and thermal structures in transitional boundary layers. *Exp. Therm. Fluid Sci.*, 1996, **12**, 338–351.
3. Fukagata, K., Iwamoto, K. and Kasagi, N., Contribution of Reynolds stress distribution to the skin friction in wall-bounded flows. *Phys. Fluids*, 2002, **14**, 73–76.
4. Taylor, R. P., Coleman, H. W., Hosni, M. H. and Love, P. H., Thermal boundary condition effects on heat transfer in the turbulent incompressible flat plate boundary layer. *Int. J. Heat Mass Transfer*, 1989, **32**, 1165–1174.
5. Rivir, R. B., Johnston, J. P. and Eaton, J. K., Heat transfer on a flat surface under a region of turbulent separation. *ASME J. Turbomach.*, 1994, **116**, 57–62.
6. Kasagi, N., Progress in direct numerical simulation of turbulent transport and its control. *Int. J. Heat Fluid Fl.*, 1998, **19**, 125–134.
7. Umur, H. and Karagoz, I., An investigation of external flows with various pressure gradients and surfaces. *Int. Commun. Heat Mass Transfer*, 1999, **26**, 411–419.
8. Crane, R. I. and Sabzvari, J., Heat transfer visualization and concave-wall laminar boundary layers. *ASME J. Turbomach.*, 1989, **111**, 51–56.
9. Barlow, R. S. and Johnston, J. P., Roll-cell structure in a concave turbulent boundary layer. AIAA 23rd Aerospace Sciences Meeting, Reno, Nevada, 1985, pp. 1–10.
10. Inagaki, K. and Aihara, Y., An experimental study of the transition region of the boundary layer along a concave wall. *Eur. J. Mech., B/Fluids*, 1995, **14**, 143–168.
11. Volino, R. J. and Simon, T. W., Boundary layer transition under high free-stream turbulence and strong acceleration conditions;

Part 2 – Turbulent transport results. *ASME J. Heat Transfer*, 1997, **119**, 427–432.
12. Flack, K. A. and Johnston, J. P., Near-wall flow in a three-dimensional boundary layer on the endwall of a 30° bend. *Exp. Fluids*, 1998, **24**, 175–184.
13. Ligrani, P. M., Choi, S., Schallert, A. R. and Skogerboe, P., Effects of Dean vortex pairs on surface heat transfer in curved channel flow. *Int. J. Heat Mass Transfer*, 1996, **39**, 27–37.
14. Umur, H., Concave wall heat transfer characteristics with longitudinal pressure gradients and discrete wall jets. *JSME Int. J.*, 1994, **37**, 403–412.
15. Wright, L. and Schobeiri, M. T., The effect of periodic unsteady flow on aerodynamics and heat transfer on a curved surface. *ASME J. Heat Transfer*, 1999, **121**, 22–33.
16. Umur, H., Flow and heat transfer with pressure gradients, Reynolds number and surface curvature. *Int. Commun. Heat Mass Transfer*, 2000, **27**, 397–406.
17. Muck, K. C., Hoffman, P. H. and Bradshaw, P., The effect of convex surface curvature on turbulent boundary layers. *J. Fluid Mech.*, 1985, **161**, 347–369.
18. Wang, T. and Simon, T. W., Heat transfer and fluid mechanics measurements in transitional boundary layers on convex-curved surfaces. *ASME J. Turbomach.*, 1987, **109**, 443–451.
19. Plesniak, M. W., Mehta, R. D. and Johnston, J. P., Curved two-stream turbulent mixing layers: Three dimensional structure and streamwise evolution. *J. Fluid Mech.*, 1994, **270**, 1–50.
20. Webster, D. R., Degraaff, D. B. and Eaton, J. K., Turbulence characteristics of a boundary layer over a two-dimensional bump. *J. Fluid Mech.*, 1996, **320**, 53–69.
21. Ligrani, P. M. and Hedlund, C. R., Transition to turbulent flow in curved and straight channels with heat transfer at high dean numbers. *Int. J. Heat Mass Transfer*, 1998, **41**, 1739–1748.
22. Cheng, K. C., Obata, T. and Gilpin, R. R., Buoyancy effects on forced convection heat transfer in the transition regime of a horizontal boundary layer heated from below. *ASME J. Heat Transfer*, 1988, **110**, 596–603.
23. So, R. M. and Mellor, G. L., Experiment on turbulent boundary layers on a concave wall. *Aeronaut. Q.*, 1975, **26**, 25–40.
24. Kestoras, M. D. and Simon, T. W., Turbulent transport measurements in a heated boundary layer: Combined effects of free-stream turbulence and removal of concave curvature. *ASME J. Heat Transfer*, 1997, **119**, 413–419.
25. Kottke, V., Taylor–Görtler vortices and their effects on heat and mass transfer. 8th International Heat Transfer Conference, San Francisco, CA, 1986, pp. 13–21.
26. Turner, A. B., Hubbe-Walker, S. E. and Bayley, F. J., Fluid flow and heat transfer over straight and curved rough surfaces. *Int. J. Heat Mass Transfer*, 2000, **43**, 251–262.

Received 20 May 2004; revised accepted 26 August 2004